JCTC Journal of Chemical Theory and Computation

Article

pubs.acs.org/JCTC

Laser-Induced Demagnetization at Ultrashort Time Scales: Predictions of TDDFT

K. Krieger,[†] J. K. Dewhurst,[†] P. Elliott,[†] S. Sharma,*[,†,‡] and E. K. U. Gross[†]

[†]Max-Planck-Institut für Mikrostrukturphysik, Weinberg 2, D-06120 Halle, Germany

[‡]Department of Physics, Indian Institute for Technology−Roorkee, 247667 Uttarkhand, India

ABSTRACT: Time-dependent density functional theory (TDDFT) is implemented in an all electron solid-state code for the case of fully unconstrained noncollinear spins. We use this to study intense, short, laser pulse-induced demagnetization in bulk Fe, Co, Ni and find that demagnetization can take place on time scales of <20 fs. It is demonstrated that this form of demagnetization is a two-step process: excitation of a fraction of electrons followed by spin-flip transitions mediated by spin−orbit coupling of the remaining localized electrons. We further show that it is possible to control the moment loss by tunable laser parameters, including frequency, duration, and intensity.

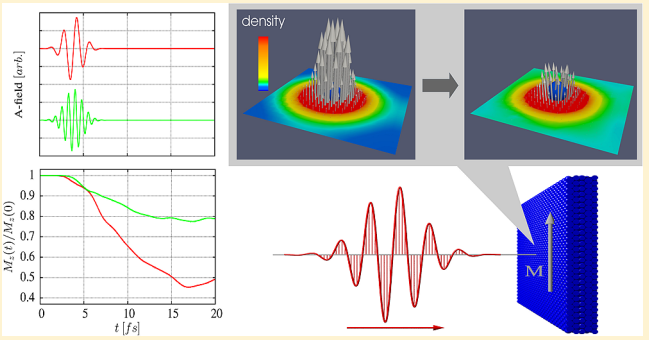

1. INTRODUCTION

Manipulation of electrons by femtosecond (fs) laser pulses opens the vast and largely unexplored physical landscape of ultrashort time scales. One possibility in this landscape is to use electronic spins, which can be optically manipulated (flipped) using lasers to store data as binary bits. The advantage of such a technique would be an increase in the speed of data storage by orders of magnitude. Ultrafast light-induced demagnetization[1] was demonstrated in the 1990s,[2] where demagnetization times (in Ni) of approximately a picosecond were achieved using intense laser pulses.[3] Recently, these demagnetization times have been measured down to 50−100 fs owing to advances made in the refinement of various experimental techniques.[2,4−13] However, we are still far from achieving the extraordinary promise of controlled manipulation[11] of spins for the production of useful devices. Some of the reasons for this are that (a) the underlying physical causes of laser-induced demagnetization are not well understood with many open questions remaining both theoretically[14−17] and experimentally[18,19] and that (b) the pulses required for controlled spin dynamics at even shorter time scales (which would be advantageous for devices) are shorter than those presently used.

The theoretical approaches to study this light matter interaction-induced ultrafast loss of moment are many and varied: the three temperature model[20] is the simplest phenomenological model that may be parametrized in order to fit the experimental data very well. This model is based on the fact that electronic charge dynamics, electronic spin dynamics, and nuclear dynamics are governed by three well-separated time scales. The model, however, does not make any statements/assumptions about the underlying physical mechanisms. Superdiffusive spin transport, where excited electrons carry spin with them from one part of the sample to another,[21,22] has been successful in describing some experiments.[23] However, recent experiments[18,19] have questioned its validity in some cases. Other proposed mechanisms include ultrafast thermal heating of electrons,[24] direct coupling between spins and carriers,[25] combined action of spin−orbit coupling, interactions between spins and laser photons,[26] higher order relativistic corrections,[27] ultrafast magnon generation,[28,29] phonons, and the Elliott−Yafet mechanism.[30,31] All these studies have in common that they describe the dynamics of the *excited electrons* using parametrized model systems and, to explain existing experimental trends, most of the calculations are performed over long time scales (i.e., at least a few hundred fs).

Keeping in mind the goal of controlled spin-dynamics at ultrashort (tens of fs) time scales, in the present work, we preempt such experiments. By using such short pulses, we can concentrate on purely electronic processes and safely neglect the influence of phonons, impurity scattering, and radiative effects on the dynamics. To have predictive power, it is essential to have a theoretical framework that is fully ab initio, which makes no assumptions about the material and mechanism leading to spin-dynamics. Time-dependent density functional theory (TDDFT),[32] which extends density functional theory into the time domain, is a formally exact method for describing such spin (and charge) dynamics under the influence of an external field, such as the vector potential of the applied laser pulse. The advantage of such a technique is clear: it does not require any empirical parameters, is fully ab initio, and is not only linear but also includes all nonlinear processes naturally as part of the simulation.

Received: June 30, 2015
Published: August 26, 2015

DOI: 10.1021/acs.jctc.5b00621
J. Chem. Theory Comput. 2015, 11, 4870−4874

In the present work, we use spin-resolved TDDFT to study the process of laser-induced demagnetization. Magnetic noncollinearity can be a major contributor in the loss of moment, so to include such effects, we extended TDDFT to the fully unconstrained noncollinear case. We have further implemented this fully unconstrained noncollinear magnetic time propagation for periodic systems in an all-electron code.[33] Several bulk systems (Fe, Co, and Ni) are studied using this code to explore various possible demagnetization scenarios. With optimal control of spins in mind, we have also explored the effect of various tunable laser parameters on the process of demagnetization.

Our analysis shows that at ultrashort time scales the demagnetization occurs as a two-step process, where the electrons first make optically induced transitions to excited states followed by spin-flip transitions mediated by spin−orbit interactions. By utilizing very short, very intense laser pulses, we can distinguish these two processes that would otherwise happen concurrently. With this information in hand, we take a step toward pulse design by studying the effect of various laser parameters on the demagnetization.

2. METHODOLOGY

The Runge−Gross theorem[32] establishes that the time-dependent external potential is a unique functional of the time-dependent density given the initial state. On the basis of this theorem, a system of noninteracting particles can be chosen such that the density of this noninteracting system is equal to that of the interacting system *for all times*. The wave function of this noninteracting system is represented as a Slater determinant of single-particle orbitals. In what follows, we shall employ the noncollinear spin-dependent version of these theorems. Then, the time-dependent Kohn−Sham (KS) orbitals are Pauli spinors determined by the equations

$$i\frac{\partial\psi_j(\mathbf{r},t)}{\partial t} = \left[\frac{1}{2}\left(-i\nabla + \frac{1}{c}\mathbf{A}_{\mathrm{ext}}(t)\right)^2 + v_s(\mathbf{r},t) + \frac{1}{2c}\boldsymbol{\sigma}\cdot\mathbf{B}_s(\mathbf{r},t) + \frac{1}{4c^2}\boldsymbol{\sigma}(\nabla v_s(\mathbf{r},t)\times -i\nabla)\right]\psi_j(\mathbf{r},t) \quad (1)$$

where $\mathbf{A}_{\mathrm{ext}}(t)$ is the vector potential representing the applied laser field, and $\boldsymbol{\sigma}$ are the Pauli matrices. The KS effective potential $v_s(\mathbf{r},t) = v_{\mathrm{ext}}(\mathbf{r},t) + v_{\mathrm{H}}(\mathbf{r},t) + v_{\mathrm{xc}}(\mathbf{r},t)$ is decomposed to the external potential v_{ext}, the classical electrostatic Hartree potential v_{H}, and the exchange-correlation (XC) potential v_{xc}. Similarly, the KS magnetic field is written as $\mathbf{B}_s(\mathbf{r},t) = \mathbf{B}_{\mathrm{ext}}(t) + \mathbf{B}_{\mathrm{xc}}(\mathbf{r},t)$, where $\mathbf{B}_{\mathrm{ext}}(t)$ is the magnetic field of the applied laser pulse plus possibly an additional magnetic field, and $\mathbf{B}_{\mathrm{xc}}(\mathbf{r},t)$ is the XC magnetic field. The final term of eq 1 is the spin−orbit coupling term. Because the wavelength of the applied laser in the present work is much greater than the size of a unit cell, we apply the dipole approximation and thus disregard the spatial dependence of the vector potential.

The XC potential has a functional dependence on the density and the magnetization density of the system at the current and all previous times. Hence, it includes the information about the whole history of this time propagation. Knowledge of this functional would solve all time-dependent (externally driven) interacting problems. In practice, however, the XC potential is always approximated. In the present work, we use the noncollinear version[34] of the adiabatic local spin density approximation (ALSDA).[35] Using the method outlined above, various extended magnetic systems are studied[36] using the full-potential linearized augmented plane wave (FP-LAPW) method[37] implemented within the Elk code.[33,38]

3. RESULTS

Presented in the middle panel of Figure 1 are the magnetic moments of bulk Fe, Co, and Ni as a function of time under the influence of an intense laser pulse.[39] In all cases, demagnetization is observed. The largest loss of moment is for Ni (43%), and the smallest is for Fe (12%). We observe that in all three cases the systems do not become noncollinear in the sense that the loss of moment in the *z*-direction would be gained in the *x*- or *y*-direction. It may be argued that because these calculations are performed using a single atom unit cell with periodic boundary conditions, it is premature to make any conclusions about the contribution of noncollinearity to the loss in moment. Hence, we have studied the effect of the same laser pulse on a Ni unit-cell 4× as large in size. So as not to bias our calculations toward collinearity, we start (at 0 fs) from a random configuration of spins with respect to one another in this supercell, and the results for the moment (per Ni atom) projected in the *x*-, *y*-, and *z*-directions are presented in the lower panel of Figure 1. Although it is essential that noncollinearity is included in the calculation (due to the presence of the spin−orbit coupling term in eq 1), we find that long-range noncollinearity, like the relative alignment of moments between atomic sites or magnons, does not play a significant role. This is mostly due to the fact that for the small time scales of interest in the present work one does not expect low energy noncollinear processes like magnons or spin-waves to dominate. Note that in all cases the magnetization remains close to the respective final value with small oscillations around this point, no remagnetization is observed on this time scale. These oscillations are a result of small short-range noncollinearity of spins.

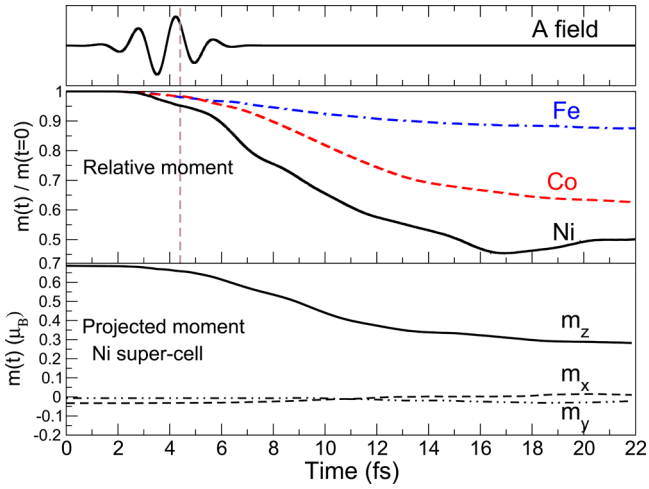

Figure 1. Top panel: **A**(t) of the laser pulse.[39] Middle panel: relative magnetic moment. Lower panel: *x*-, *y*-, and *z*-projected magnetic moments per atom for a supercell of Ni.

A feature of the demagnetization process in all three cases (Fe, Co, and Ni) is that the majority of the demagnetization occurs *after* the maximum of the laser pulse. We refer to this effect as a time lag between the laser pulse and the demagnetization. Note that we can only distinguish this effect by using such a short pulse, and for longer pulses, the two

DOI: 10.1021/acs.jctc.5b00621
J. Chem. Theory Comput. 2015, 11, 4870−4874

processes become mixed with each other and cannot be cleanly separated.

The question now arises: what is the origin of this time lag and what causes the demagnetization? To understand this, we plot in Figure 2 two contributions to the moment for Ni. They

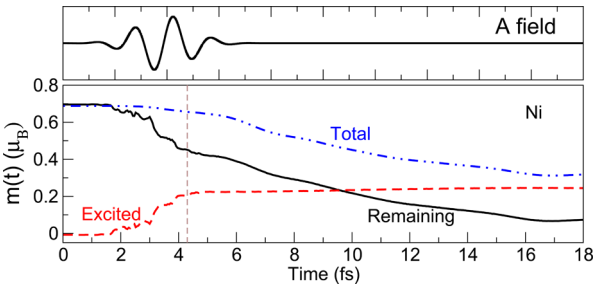

Figure 2. Upper panel: **A**(t) of the laser pulse.[39] Lower panel: total magnetic moment, magnetic moment coming from excited, and remaining electrons for Ni.

are (a) from the electrons, which under the influence of the intense laser pulse make a transition to excited states and become delocalized, and (b) from the remaining electrons, which are localized close to the nuclei. These fractions can be easily calculated within the LAPW method where the space is divided into muffin tins and an interstitial region; the localized moment is calculated by integrating the magnetization density over a small muffin-tin sphere around each nucleus and subtracting this from the total moment to give the remaining contribution.

During the first ∼5 fs, the electrons, carrying their spins, make transitions to excited states. This leads to an increase in the total moment associated with the excited electrons and to a lowering of the moment coming from the remaining localized electrons such that the sum of the two moments stays almost constant. Note that this initial excitation is strongly nonlinear and depends on the electronic band structure of the material. After ∼5 fs, the moment of the excited delocalized electrons stays almost constant, whereas some of the remaining localized electrons make spin-flip transitions, leading to a loss in the total moment. Hence, the demagnetization mechanism is clearly a two step process: (1) during the first ∼5 fs, a fraction of the electrons become delocalized by making transitions to the excited states; (2) this is followed by the remaining localized electrons making spin-flip transitions. The major factor responsible for these spin-flip transitions of the localized electrons is the spin−orbit coupling term in eq 1. To confirm this fact, we also performed similar calculations in which the spin−orbit coupling term was set to zero and find no such demagnetization.

In the past, using a two band model, spin−orbit mediated spin-flip has already been identified as an important contributor to the demagnetization process.[26] What sets the present work apart is not just its ab initio nature but also the fact that we have explored all three kinds of spin excitations mediated by spin−orbit coupling: magnons, intersite noncollinearity, and spin-flips. Despite this, we find spin-flips to be the major cause of demagnetization. The magnitude and speed of this demagnetization are much greater than those seen in previous works.[27,40−43]

The analysis listed above scrutinizes the process of demagnetization. What is most important for future technological applications is not just this knowledge but also the means to manipulate spins in a controlled manner. We now show the effect of the three easily tunable parameters of a laser pulse: intensity, frequency, and duration on the demagnetization. In the upper panel of Figure 3 is shown the magnetic

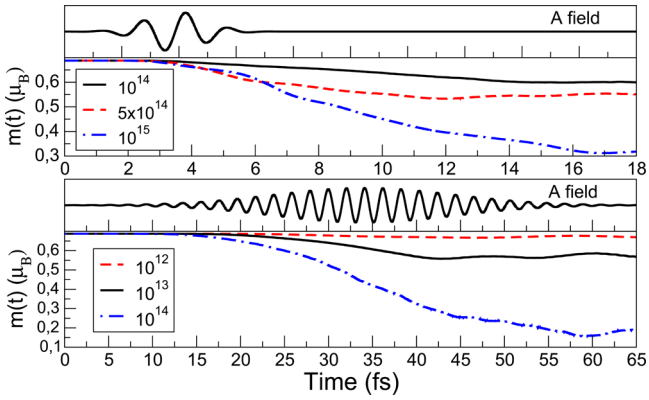

Figure 3. Top and third panel: **A**(t) of the laser pulse. Second panel: magnetic moment for bulk Ni under the influence of 6 fs (fwhm = 2.2 fs) laser pulses[44] with different peak intensities. Fourth panel: magnetic moment for bulk Ni under the influence of 60 fs (fwhm = 17 fs) laser pulses[45] with different peak intensities.

moment for Ni as a function of the peak intensity.[44] The effect of intensity on the demagnetization is dramatic. For a pulse of peak intensity 10^{15} W/cm^2, 50% of the moment is lost after 20 fs whereas only 14% loss is observed for a pulse of peak intensity 10^{14} W/cm^2. We note that at these intensities the response of the system is far from linear and that nonlinear effects are predominant.

In all of these studies, a very short laser pulse of 6 fs (fwhm = 2.2 fs) was applied.[44] Most experiments are currently limited to using much longer laser pulses (shortest pulse being ∼120−300 fs (fwhm = 50−80 fs)). In the lower panel of Figure 3, we show the effect of a longer pulse of varying intensities.[45] We again find that the demagnetization increases with increasing intensity. For longer pulse durations, a higher demagnetization, with 71% loss in moment induced by the pulse of peak intensity 10^{14} W/cm^2, is observed. Figure 3 clearly shows that, for longer duration pulses, a lower intensity is sufficient to obtain large demagnetization.

The magnetic moment also shows a strong dependence on the carrier frequency of the pulse. In Figure 4 are presented the results for short laser pulses with varying frequency. It is clear that the central frequency of the pulse can also be used to control the amount of demagnetization. The dependence of demagnetization on frequency is nonlinear and can be tuned to obtain a loss in moment of between 20 and 53% for bulk Ni. The ideal frequency needed to achieve maximum moment loss (or rather at which the system becomes most absorptive) is a material-dependent property and is related to the details of the band structure. This fact also explains the results in Figure 1, where the chosen frequency is better suited for Ni and Co than for Fe. It is also important to mention the effect of yet another laser parameter, namely, the polarization of the pulse. In the present work, linearly polarized light in the *x*-direction was used (perpendicular to the direction of the moment, which points along the *z*-axis). We find that changing the plane of polarization of this linearly polarized light[47] does not affect the process of demagnetization for such short pulses. In the

DOI: 10.1021/acs.jctc.5b00621
J. Chem. Theory Comput. 2015, 11, 4870−4874

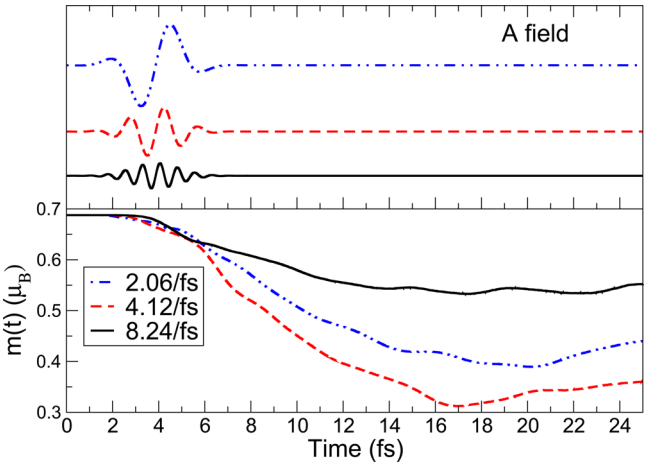

Figure 4. Top panel: **A**(t) of the laser pulses[46] of peak intensity 10^{15} W/cm^2 and varying frequency. Lower panel: magnetic moment (in Bohr magneton) under the influence of the laser pulses in the top panel.

future, it would be interesting to study the effect of circularly polarized light on the process of demagnetization[48]

4. CONCLUSIONS

In the present work, we show predictions of demagnetization made by the fully ab initio method of TDDFT for ultrashort laser pulses interacting with the bulk ferromagnets of Fe, Ni, and Co. The significant feature of our results is that the demagnetization occurs on very short time scales on the order of a few tens of femtoseconds. Furthermore, we demonstrate the possibility of control of the spin moments in solids by studying the effect of easily tunable laser parameters, such as the duration, intensity, and frequency on the process of moment loss in Ni. Control of the magnetic moment on such a short time scale is of vital importance to future technological transfer of these processes, which are several orders of magnitude faster than currently available commercial devices. It is only with a first-principles approach to simulating electron dynamics, and the optical excitation in particular, that these results could have been obtained. We also demonstrated that demagnetization is a two-step process with excitation of a fraction of the electrons followed by spin-flip transitions of the remaining localized electrons. Disentangling the two processes was only possible when using ultrashort pulses. With these predictions we hope to stimulate such short-time, intense laser pulse experiments to elucidate the exact nature of spin-light interaction.

AUTHOR INFORMATION

Corresponding Author

*E-mail: sharma@mpi-halle.mpg.de.

Notes

The authors declare no competing financial interest.

REFERENCES

(1) Agranat, M. B.; Ashitkov, S. I.; Granovskii, A. B.; Rukman, G. I. *Sov. Phys. JETP* **1984**, *59*, 804.
(2) Beaurepaire, E.; Merle, J.-C.; Daunois, A.; Bigot, J.-Y. *Phys. Rev. Lett.* **1996**, *76*, 4250.
(3) Vaterlaus, A.; Beutler, T.; Guarisco, D.; Lutz, M.; Meier, F. *Phys. Rev. B: Condens. Matter Mater. Phys.* **1992**, *46*, 5280.
(4) Hohlfeld, J.; Matthias, E.; Knorren, R.; Bennemann, K. H. *Phys. Rev. Lett.* **1997**, *78*, 4861.
(5) Scholl, A.; Baumgarten, L.; Jacquemin, R.; Eberhardt, W. *Phys. Rev. Lett.* **1997**, *79*, 5146−5149.
(6) Aeschlimann, M.; Bauer, M.; Pawlik, S.; Weber, W.; Burgermeister, R.; Oberli, D.; Siegmann, H. C. *Phys. Rev. Lett.* **1997**, *79*, 5158.
(7) Hohlfeld, J.; Güdde, J.; Dühr, U. C. O.; Korn, G.; Matthias, E. *Appl. Phys. B: Lasers Opt.* **1999**, *68*, 505.
(8) Regensburger, H.; Vollmer, R.; Kirschner, J. *Phys. Rev. B: Condens. Matter Mater. Phys.* **2000**, *61*, 14716−14722.
(9) Guidoni, L.; beaurepaire, E.; Bigot, J. Y. *Phys. Rev. Lett.* **2002**, *89*, 017401.
(10) Schmidt, A. B.; Pickel, M.; Wiemhöfer, M.; Donath, M.; Weinelt, M. *Phys. Rev. Lett.* **2005**, *95*, 107402.
(11) Kirilyuk, A.; Kimel, A. V.; Rasing, T. *Rev. Mod. Phys.* **2010**, *82*, 2731−2784.
(12) Melnikov, A.; Razdolski, I.; Wehling, T. O.; Papaioannou, T. E.; Roddatis, V.; Fumagalli, P.; Aktsipetrov, O.; Lichtenstein, A. I.; Bovensiepen, U. *Phys. Rev. Lett.* **2011**, *107*, 076601.
(13) Sultan, M.; Atxitia, U.; Melnikov, A.; Chubykalo-Fesenko, O.; Bovensiepen, U. *Phys. Rev. B: Condens. Matter Mater. Phys.* **2012**, *85*, 184407.
(14) Zhang, G. P.; Hübner, W.; Lefkidis, G.; Bai, Y.; George, T. F. *Nat. Phys.* **2009**, *5*, 499.
(15) Carva, K.; Battiato, M.; Oppeneer, P. M. *Nat. Phys.* **2011**, *7*, 665.
(16) Zhang, G. P.; Hubner, W.; Lefkidis, G.; Bai, Y.; George, T. F. *Nat. Phys.* **2011**, *7*, 665.
(17) Illg, C.; Haag, M.; Fähnle, M. *Phys. Rev. B: Condens. Matter Mater. Phys.* **2013**, *88*, 214404.
(18) Schellekens, A. J.; Verhoeven, W.; Vader, T. N.; Koopmans, B. *Appl. Phys. Lett.* **2013**, *102*, 252408.
(19) Moisan, N.; Malinowski, G.; Mauchain, J.; Fullerton, E. E.; Thiaville, A. *Sci. Rep.* **2014**, *4*, 4658.
(20) Koopmans, B.; Malinowski, G.; Longa, F. D.; Steiauf, D.; Fähnle, M.; Roth, T.; Cinchetti, M.; Aeschlimann, M. *Nat. Mater.* **2010**, *9*, 259.
(21) Battiato, M.; Carva, K.; Oppeneer, P. M. *Phys. Rev. Lett.* **2010**, *105*, 027203.
(22) Rhie, H. S.; Dürr, H. A.; Eberhardt, W. *Phys. Rev. Lett.* **2003**, *90*, 247201.
(23) Eschenlohr, A.; Battiato, M.; Maldonado, P.; Pontius, N.; Kachel, T.; Holldack, K.; Mitzner, R.; Föhlisch, A.; Oppeneer, P. M.; Stamm, C. *Nat. Mater.* **2013**, *12*, 332.
(24) Ostler, T.; Barker, J.; Evans, R.; Chantrell, R.; Atxitia, U.; Chubykalo-Fesenko, O.; Moussaoui, S. E.; Guyader, L. L.; Mengotti, E.; Heyderman, L.; Nolting, F.; Tsukamoto, A.; Itoh, A.; Afanasiev, D.; Ivanov, B.; Kalashnikova, A.; Vahaplar, K.; Mentink, J.; Kirilyuk, A.; Rasing, T.; Kimel, A. *Nat. Commun.* **2012**, *3*, 666.
(25) Cywinski, L.; Sham, L. J. *Phys. Rev. B: Condens. Matter Mater. Phys.* **2007**, *76*, 045205.
(26) Zhang, G. P.; Hübner, W. *Phys. Rev. Lett.* **2000**, *85*, 3025−3028.
(27) Bigot, J.-Y.; Vomir, M.; Beaurepaire, E. *Nat. Phys.* **2009**, *5*, 515.
(28) Schmidt, A. B.; Pickel, M.; Donath, M.; Buczek, P.; Ernst, A.; Zhukov, V. P.; Echenique, P. M.; Sandratskii, L. M.; Chulkov, E.; Weinelt, M. *Phys. Rev. Lett.* **2010**, *105*, 7197401.
(29) Haag, M.; Illg, C.; Fähnle, M. *Phys. Rev. B: Condens. Matter Mater. Phys.* **2014**, *90*, 014417.
(30) Koopmans, B.; Ruigrok, J. J. M.; Longa, F. D.; de Jonge, W. J. M. *Phys. Rev. Lett.* **2005**, *95*, 267207.
(31) Koopmans, B. *Nat. Mater.* **2007**, *6*, 715.
(32) Runge, E.; Gross, E. K. U. *Phys. Rev. Lett.* **1984**, *52*, 997−1000.
(33) Dewhurst, J. K.; et al. http://elk.sourceforge.net, 2004.
(34) Kubler, J.; Hock, K.-H.; Sticht, J.; Williams, A. R. *J. Phys. F: Met. Phys.* **1988**, *18*, 469.
(35) Zangwill, A.; Soven, P. *Phys. Rev. Lett.* **1980**, *45*, 204−7.
(36) In all cases, a *k*-point mesh of 8 × 8 × 8 was used and 120 empty states were needed for convergence. The symmetries were not used to reduce the *k*-point set. The time between 0 and 30 fs was

DOI: 10.1021/acs.jctc.5b00621
J. Chem. Theory Comput. 2015, 11, 4870−4874

divided into a total of 48000 time steps. Lattice parameters of 3.52 Å for fcc Ni, 2.87 Å for bcc Fe, and 3.544 Å for fcc Co were used.
(37) Singh, D. J. *Planewaves Pseudopotentials and the LAPW Method*, 2nd edition; Kluwer Academic Publishers: Boston, MA, 1994; pp 55−108.
(38) Dewhurst, J. K.; Krieger, K.; Sharma, S.; Gross, E. K. U. http://arxiv.org/abs/1412.0996, 2015.
(39) The pulse duration (time between the start and the end of the pulse) is 6 fs, the peak intensity is 10^{15} W/cm^2, the frequency is 4.12/fs, and the fluence is 934.8 mJ/cm^2. The pulse is linearly polarized along the *x*-axis perpendicular to the direction of the moment.
(40) Boeglin, C.; Beaurepaire, E.; Halté, V.; López-Flores, V.; Stamm, C.; Pontius, N.; Dürr, H. A.; Bigot, J.-Y. *Nature* **2010**, *465*, 458.
(41) Popova, D.; Bringer, A.; Blügel, S. *Phys. Rev. B: Condens. Matter Mater. Phys.* **2011**, *84*, 214421.
(42) Stamm, C.; Pontius, N.; Kachel, T.; Wietstruk, M.; Dürr, H. A. *Phys. Rev. B: Condens. Matter Mater. Phys.* **2010**, *81*, 104425.
(43) Popova, D.; Bringer, A.; Blügel, S. *Phys. Rev. B: Condens. Matter Mater. Phys.* **2012**, *85*, 094419.
(44) The pulse duration (time between the start and the end of the pulse) is 6 fs, and the frequency is 4.12/fs. The pulse is linearly polarized along the *x*-axis perpendicular to the direction of the moment. The fluence is 934.8, 467.5, and 93.5 mJ/cm^2 for the pulse of peak intensities of 10^{15}, 5×10^{14}, and 10^{14} W/cm^2, respectively.
(45) The pulse duration (time between the start and the end of the pulse) is 60 fs, and the frequency is 3.03/fs. The pulse is linearly polarized along the *x*-axis perpendicular to the direction of the moment. The fluence is 913.5, 92.6, and 9.3 mJ/cm^2 for the pulse of peak intensities of 10^{14}, 10^{13}, and 10^{12} W/cm^2, respectively.
(46) The pulse duration (time between the start and the end of the pulse) is 6 fs, and the peak intensity is 10^{15} W/cm^2. The pulse is linearly polarized along the *x*-axis perpendicular to the direction of the moment. The fluence is 1009.4, 934.8, and 915.9 mJ/cm^2 for the pulse of frequency 2.06, 4.14, and 8.24/fs, respectively.
(47) Longa, F. D.; Kohlhepp, J. T.; de Jonge, W. J. M.; Koopmans, B. *Phys. Rev. B: Condens. Matter Mater. Phys.* **2007**, *75*, 224431.
(48) Hansteen, F.; Kimel, A.; Kirilyuk, A.; Rasing, T. *Phys. Rev. B: Condens. Matter Mater. Phys.* **2006**, *73*, 014421.

DOI: 10.1021/acs.jctc.5b00621
J. Chem. Theory Comput. 2015, 11, 4870−4874